Modeling and Control of a Spark Ignition Engine with Variable Cam Timing

A. G. Stefanopoulou*, J. A. Cook†, J. S. Freudenberg*,
J. W. Grizzle*, M. Haghgooie†, and P. S. Szpak†

Abstract

A control scheme is designed to minimize emissions and respond to rapid throttle changes in a fuel injected, spark ignition engine equipped with variable cam timing. The model is derived from engine mapping data for an eight cylinder experimental engine mounted in a dynamometer test cell; it is fundamentally nonlinear and multivariable. The control scheme jointly manages fuel and cam position.

1 Introduction.

Modern automobile engines must satisfy the challenging and often conflicting goals of minimizing exhaust emissions, providing increased fuel economy and satisfying driver performance requirements over a wide range of operating conditions. An innovative mechanical design approach to achieving these goals has been the development of variable cam timing (VCT) engines.

It is well known that cam timing can inhibit the production of oxides of nitrogen (NOx) and reduce the amount of unburned hydrocarbons (HC) emitted to the exhaust system [5]. By retarding the cam timing, combustion products which would otherwise be expelled during the exhaust stroke are retained in the cylinder during the subsequent intake stroke. The contribution of this diluent to the mixture in the cylinder reduces the combustion temperature and suppresses NOx formation. In addition, this process often reduces HC emissions since the internally recirculated exhaust gas subjected to the additional combustion cycle is generally from the crevice volumes at the piston/cylinder wall interface and is rich in unburned HC. The effect is to reduce the base HC and NOx emission levels of the engine with respect to a conventional powerplant, resulting in lower tailpipe emissions at equivalent catalytic converter efficiencies. Of course, VCT obviates the requirement for external exhaust gas recirculation (EGR) systems commonly used for NOx reduction.

*Control Systems Laboratory, Department of Electrical Engineering and Computer Science, University of Michigan, Ann Arbor, MI 48109-2122; work supported in part by the National Science Foundation under contract NSF ECS-92-13551; matching funds to this grant were provided by FORD MO. CO.

†Ford Motor Company, Scientific Research Laboratory, PO Box 2053, Mail Drop 1170 SRL, Dearborn, MI 48121-2053

One type of VCT engine utilizes a hydraulically actuated mechanism to rotate the camshaft relative to the crankshaft and advance the valve timing with respect to the engine induction and exhaust strokes. This is illustrated in the valve lift profiles shown in Figure 1.

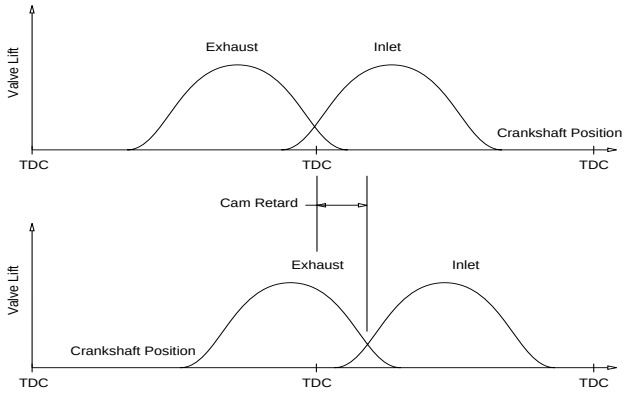

Figure 1: Valve lift profiles.

The goal of the current work is threefold: (i) maintain steady state and transient air fuel ratio (A/F) at stoichiometry, (ii) minimize feedgas NOx and HC emissions, and (iii) provide satisfactory torque response to meet vehicle and customer performance requirements during changes in throttle position. Rapid throttle movements reflect the driver's demand for changes in torque and vehicle acceleration, and strongly influence the cylinder air charging process, mixture formation and transient performance of the engine. For both HC and NO_x emissions, the primary control objective is to maintain the A/F at stoichiometry at all times since this corresponds to the point of maximum efficiency of the catalytic converter. The additional complexity is that rapid throttle movements imposed by the driver are now accompanied with changes in cam phasing in order to minimize the amount of NO_x and HC in the feedgas. Both throttle and cam phasing can rapidly affect transient and steady state A/F and thereby make the task of A/F control even more challenging.

The identified model for the VCT engine is described in the next section. Section 3 discusses the control design. Simulation examples, results and comparisons are

presented in Section 4.

2 Engine Model.

The engine model used in this study is a continuous, nonlinear, low-frequency, phenomenological representation of an eight cylinder experimental VCT engine, based on [2], with appropriate modifications for variable cam timing.

The throttle body, engine pumping rate, torque generation and NOx and HC emissions are included as nonlinear static algebraic relations. Their parameters are determined from regressed engine steady state data using a least squares approach. Physically based differential and difference equations are used to describe the dynamic elements of the engine, such as inlet manifold pressure and the delays in the signal paths. The identification of these parameters is based on the dynamic response of the experimental engine to small step inputs. Furthermore, the model includes actuator and sensor dynamics, and some important computational delays. The following subsections describe each of the engine components, and at the end of the section the identified model is validated against actual engine data.

2.1 Breathing Process.

The manifold acts as a plenum, and its dynamics can be described by the following first order differential equation that relates the rate of change of the manifold pressure (P_m) to the flow rates into and out of the manifold ($\dot{m}_\theta$ and $\dot{m}_{cyl}$ respectively)

$$\frac{d}{dt}P_m = K_m(\dot{m}_\theta - \dot{m}_{cyl}), \text{ where } K_m = \frac{R \cdot T}{V_m} \quad (2.1)$$

The constant $K_m = 0.12\frac{bar}{g}$ has been identified from dynamic experimental data and compared with its physically based value [3].

The mass air flow rate into the manifold ($\dot{m}_\theta$) through the primary throttle body is a function of throttle angle (θ), the upstream pressure (P_o), which we assume to be atmospheric, i.e. $P_o = 1$ bar, and the downstream pressure, which is the manifold pressure (P_m). The function describing $\dot{m}_\theta$ is given in [6] by

$$\begin{aligned} \dot{m}_\theta &= g_1(P_m) \cdot g_2(\theta) \\ g_1(P_m) &= \begin{cases} 1 & \text{if } P_m \le P_O/2 \\ \frac{2}{P_O}\sqrt{P_m P_O - P_m^2} & \text{if } P_m > P_O/2 \end{cases} \\ g_2(\theta) &= F(1, \theta, \theta^2, \theta^3) \end{aligned} \quad (2.2)$$

where $g_2(\theta)$ is a third order polynomial[1] of throttle angle.

The engine pumping mass air flow rate ($\dot{m}_{cyl}$) is a function of the cam phasing (CAM), the manifold pressure (P_m), and the engine speed (N). The resulting polynomial[1] is of degree three, and a third order polynomial in each individual variable :

$$\begin{aligned} \dot{m}_{cyl} = \quad & F(1, CAM, CAM^2, CAM^3, \\ & P_m, P_m^2, P_m^3, N, N^2, N^3) \end{aligned} \quad (2.3)$$

[1] Due to space limitations the exact polynomials or algebraic relations are omitted, but can be obtained from the first author.

Figure 2 shows the variation of mass air flow rate with manifold pressure (P_m) for different values of cam phasing (CAM) at constant engine speed (1000 RPM).

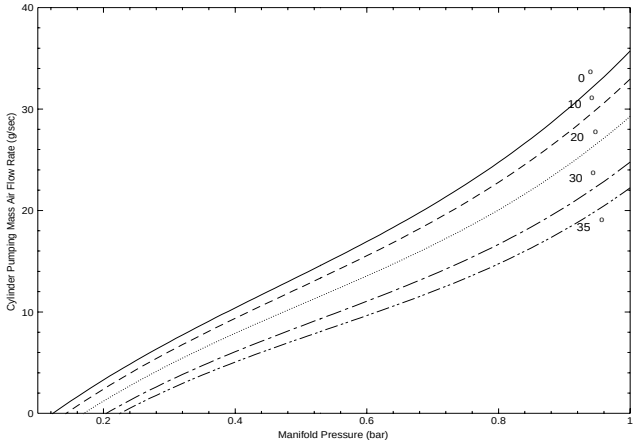

Figure 2: Engine pumping mass air flow rate .

2.2 Torque Generation.

Engine torque (T_q) was mapped as a function of the cylinder air charge (CAC), the air fuel ratio (A/F), and the engine speed (N). We assumed uniform pulse, homogeneous charge, and spark scheduling to achieve maximum best torque (MBT). The modeled torque equation[1] is a polynomial of degree three, and a third order polynomial in each individual variable :

$$\begin{aligned} T_q = \quad & F(1, CAC, CAC^2, CAC^3, \\ & A/F, A/F^2, A/F^3, N, N^2, N^3) \end{aligned} \quad (2.4)$$

The variation of torque with A/F for different values of cylinder air charge (grams per intake-event) at constant engine speed (1500 RPM) is shown in Figure 3.

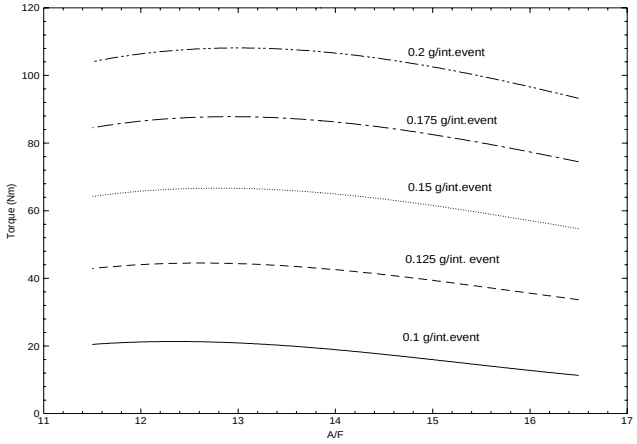

Figure 3: Engine Torque.

2.3 NOx and HC emissions.

The steady state NOx and HC emissions depend on engine speed (N), cam phasing (CAM), air fuel ratio (A/F), and manifold pressure (P_m). The four variable

regression applied in the NOx emission data resulted in an eighth degree polynomial. The modeled NOx equation [1] is a second, first, third and second order polynomial of engine speed (N), cam phasing (CAM), air fuel ratio (A/F), and manifold pressure (P_m) respectively :

$$\begin{aligned} NOx = \quad & F_1(1, N, N^2) \cdot F_2(1, CAM) \cdot \\ & F_3(1, A/F, A/F^2, A/F^3) \cdot \\ & F_4(1, P_m, P_m^2) \end{aligned} \tag{2.5}$$

The emitted amount of HC increases sharply as manifold pressure P_m decreases. For this reason the modeled HC emission equation is a polynomial of the engine speed(N), cam phasing (CAM), air fuel ratio (A/F), and inverse manifold pressure ($\frac{1}{P_m}$). Observing the data trend led us to include a term of modulated cam phasing ($\frac{CAM}{P_m \frac{1}{16}}$), which significantly improved the statistical measures. The function[1] describing HC emissions is described by

$$\begin{aligned} HC = \quad & F_1(1, N, N^2) F_2(1, A/F, A/F^2) \cdot \\ & F_3(1, \tfrac{1}{P_m}) + F_4(1, CAM \tfrac{CAM}{P_m \frac{1}{16}}) \end{aligned} \tag{2.6}$$

Figure 4 shows the variation of NOx and HC emissions with cam phasing at constant air fuel ratio, manifold pressure, and engine speed ($A/F = 14.64$, $P_m = 0.4$ bar, and $N = 2000$ RPM).

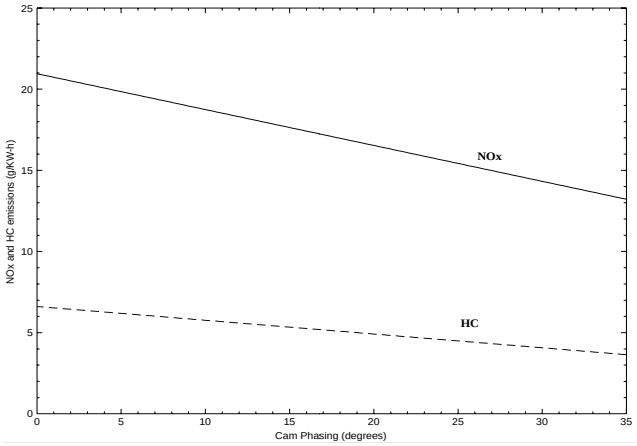

Figure 4: NOx and HC emission.

2.4 Process Delays.

The discrete nature of the engine causes delays in the signal path. For the engine studied, 360 degrees of induction-to-power stroke delay is assumed. We should note here that even though we cannot measure torque, we are using its modeled value as a performance variable together with NOx and HC emissions in the control design. The NOx and HC emissions are steady state measurements (average values) and cannot be measured in a dynamic manner. Their identified static nonlinear maps (section 2.3), however, will be included in the VCT model in the same dynamic manner as the torque generation function.

A delay of 810 degrees is also identified between the mass charge formation and the time when its corresponding exhaust gas reaches the EGO sensor. To achieve good combustion properties, the computed fuel is injected on closed intake valves, i.e. during the exhaust stroke prior to the intake event. Including the computational delay involved in the fuel pulse width calculation, we estimated a total of 180 degrees of delay between the commanded fuel pulse width and the formation of its corresponding charge.

2.5 Actuators and Sensors.

The dynamics of the VCT actuator have been identified and are described by the following transfer function

$$\frac{CAM_{actual}}{CAM_{commanded}} = \frac{-0.706s + 705.8}{s^2 + 16.13s + 705.8} \tag{2.7}$$

Also, a reduced order model has been developed for the same actuator for control purposes, and is given by

$$\frac{CAM_{actual}}{CAM_{commanded}} = \frac{-0.013s + 26.959}{s + 26.959} \tag{2.8}$$

The dynamics of the EGO sensor are modeled as a first order lag followed by a preload (i.e. relay or switching-type) nonlinearity, which we will overlook in the current control design. The time constant of the EGO sensor is typically 70 msec.

A hot wire anemometer is used to measure the mass air flow rate through the throttle body. A first order lag with time constant equal to 27 msec is used to describe the air meter dynamics. Finally, cam phasing measurements are received with a delay of 90 degrees.

2.6 Model Validation.

The test work here involves the comparison of the identified model response with actual engine data to small step inputs. Figure 5 shows the response of manifold pressure (P_m), measured mass air flow (MAF), and the generated torque (T_q) to a step change in throttle position. Figure 6 shows the response of the actual cam position (CAM), manifold pressure (P_m) and generated torque (T_q) to a step change in cam position.

3 Control Design.

The control oriented model developed has two actuators: the fuel injector pulse widths (F_c) and the cam position (CAM_c). The measured outputs are: air fuel ratio (A/F) at the EGO sensor, the mass air flow (MAF), engine speed (N), and cam phasing (CAM_m). The goal of the control design is to keep emisions as low as possible, by maintaining air fuel ratio (A/F) close to stoichiometry, and minimizing feedgas NOx and HC emissions, while providing good driveability during rapid throttle movements in a VCT engine.

Performance variables are NOx and HC emissions, and the rate of change of the engine torque during the throttle changes. Here we are considering the basic customer performance requirement: the torque response of

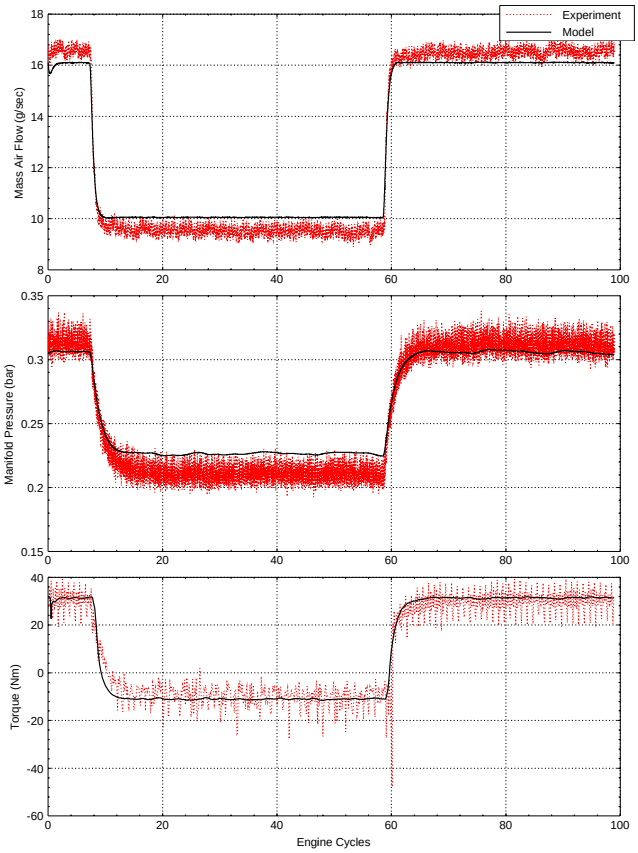

Figure 5: Model and engine actual dynamic response to throttle step command

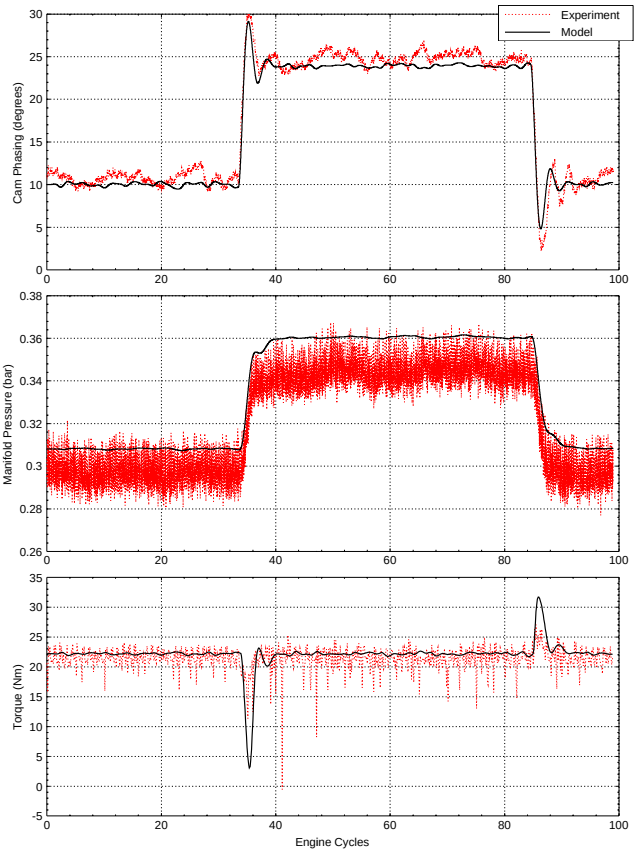

Figure 6: Model and engine actual dynamic response to cam phasing step command

the engine. Variable cam timing can alter the speed of torque response of the engine, and the control scheme must wisely schedule the cam phasing. On the other hand, satisfying low NOx and HC emissions is straightforward, as can be seen in Figure 4 by using the maximum cam phasing whenever possible. Based on these requirements, the designed (for constant engine speed) steady state cam phasing is a function of throttle position (θ): near idle, it is scheduled for idle stability, at mid-throttle, it is scheduled for emissions, and at wide open thottle (WOT), it is scheduled for maximum torque. Figure 7 shows the steady state cam phasing for engine speed equal to 2000 RPM. The transition of the cam phasing between set-points during rapid throttle changes is a crucial parameter to the control design. Precise A/F control favors slow cam phasing transients; minimum feedgas NOx and HC emissions require instantaneous change of the cam position to the scheduled set-point.

An LQG/LTR design methodology is developed to rigorously undertake the trade-off between catalytic converter performance and feedgas emissions. The multivariable controller is designed to track the desired cam phasing (value from the feedforward map) and maintain A/F at stoichiometry. Due to the large inherent delay between the injection process and the time its associated air fuel charge passes by the EGO sensor, the A/F feedback signal does not permit high enough bandwidth to accomodate fast transients. Utilizing the measured mass air flow (MAF), and the measured cam position (CAM_m), we designed a feedforward control scheme. The advantage of the resulting two degrees of freedom (2DOF) control topology is that it affords greater freedom in achieving the design trade-off.

The fundamental work given in [3] is modified for the variable cam timing effects on the cylinder air charge. The task involves the estimation of the cylinder pumping mass air flow rate ($\widehat{\dot{m}_{cyl}}$) from the measured cam phasing (CAM_m), the estimated manifold pressure ($\widehat{P_m}$), and the engine speed

$$\widehat{\dot{m}_{cyl}} = P(CAM_m, \widehat{P_m}, N) \tag{3.1}$$

The estimated manifold pressure ($\widehat{P_m}$) is calculated as

$$\frac{d}{dt}\widehat{P_m} = K_m(\tau\frac{d}{dt}MAF + MAF - \widehat{\dot{m}_{cyl}}) \tag{3.2}$$

where we considered the dynamics of the mass air flow meter : $\tau\frac{d}{dt}MAF + MAF = \dot{m}_\theta$. To eliminate the derivative on the air flow measurement we use the variable $\chi = \widehat{P_m} - K_m \cdot \tau \cdot MAF$. This yields the cylinder mass

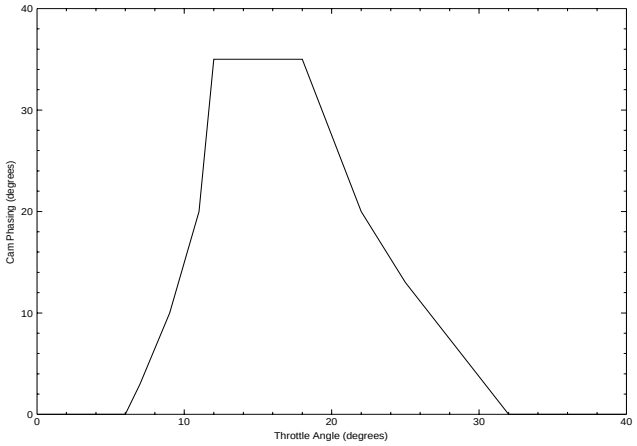

Figure 7: Steady state cam phasing

air flow rate feedforward estimator

$$\begin{aligned} \tfrac{d}{dt}\chi &= K_m(MAF - \widehat{\dot{m}_{cyl}}) \\ \widehat{P_m} &= \chi + K_m \cdot \tau \cdot MAF \\ \widehat{\dot{m}_{cyl}} &= P(CAM_m, \widehat{P_m}, N) \end{aligned} \tag{3.3}$$

4 Simulation Example

The purpose of this section is to illustrate some of the properties of the closed loop system for a conventional engine (fixed cam phasing) and the VCT engine. In the last part, we discuss the design of a PI controller and compare it with the multivariable control scheme.

Figure 8 is the simulated response of the conventional engine (fixed cam phasing) and the VCT engine to a square wave in commanded throttle. The sequence of throttle commands is 9.0 degrees (nominal) to 7.2 degrees to 12.0 degrees and back to 7.2 degrees and then to 9.0 degrees. The corresponding cam phasing set-points are 3 degrees to 10 degrees to 35 degrees (maximum) and back to 3 degrees and then to 10 degrees. The conventional engine scheme has fixed cam at 0 degrees.

The resulting torque response of the VCT engine is kept as responsive as the conventional engine, with the result that the transient A/F is slightly worse than the A/F of the conventional engine. The advantage of the VCT engine over the conventional scheme is demonstrated at the feedgas NOx and HC emissions. Using the integrated area defined by the NOx and HC emission curves as a crude measurement of engine emissions, we can estimate a possible reduction of 10% in NOx and 20% in HC during that period.

Our long term goal is to implement the control scheme on an experimental vehicle and test its performance. A natural step towards this goal is to explore a simpler control scheme. Using the design characteristics of the multivariable controller it is possible to reduce the complexity of the previously described MIMO control scheme to a SISO feedback controller. The developed controller is a PI controller that adjusts the fuel pulse width using the A/F measurement at the EGO sensor, and the previously developed feedforward term (Equation 3.3).

In section 3 we discussed the importance of the cam transient behavior to the trade-off of the design specification. The achieved transient response of the cam phasing in the multivariable methodology can be represented as a first order lag with a time constant equal to one engine cycle, which is equal to 60 msec at 2000 RPM (nominal operating engine speed). To achieve equivalent performance with the PI scheme, we used the same lowpass filter to regulate the cam transition between two set-points.

Figure 9 compares the two simulated schemes: MIMO controller versus PI controller. Similarity in the cam phasing dynamics is maintained, and the engine torque responses are almost identical. The NOx and HC emissions in both cases are equivalent, however, there is a degradation in A/F performance of the PI control scheme, which will cause an increase of the tailpipe emissions due to the sensitive performance of the three-way-catalytic (TWC) converter.

The overall design seems promising, but we should note here that the controller is based on a partly linearized engine model and it is important to have a control scheme that operates over a wide range of engine speed. The next stage of our work will be to implement the control scheme studied, and assess the emission improvements obtained with the VCT engine.

5 Acknowledgment

The authors thank M. Seaman for assembling the experimental facility and collecting the data.

References

[1] C. F. Aquino, "Transients A/F Control Characteristics of the 5 Liter Central Injection Engine," SAE Paper No. 810494, 1981.

[2] P. R. Crossley and J. A. Cook, "A Nonlinear Model for Drivetrain System Developement," IEE Conference 'Control 91', Edinburgh, U.K., March 25-28, 1991. IEE Conference Publication 332 Vol. 2, pp 921-925.

[3] J. W. Grizzle, J. A. Cook and W. P. Milam, "Improved Transient Air-Fuel Ratio Control using Air Charge Estimator," Proc. 1994 Amer. Contr. Conf., Vol. 2, pp 1568-1572, June 1994.

[4] J. Heywood, *Internal Combustion Engine Fundamentals*, McGraw Hill, 1988.

[5] G.-B. Meacham, "Variable Cam Timing as an Emission Control Tool," SAE Paper No. 700645, 1970.

[6] J. M. Novak, "Simulation of the Breathing Process and Air-Fuel Ratio Distribution Characteristics of Three-Valve, Stratified Charge Engines," SAE Paper No. 770881, 1977.

[7] B. K. Powell, and W. F. Powers, "Linear Quadratic Control Design for Nonlinear IC Engine Systems," Proc. International Society of Automotive Technology and Automation, Stockholm, Sweden, 1981.

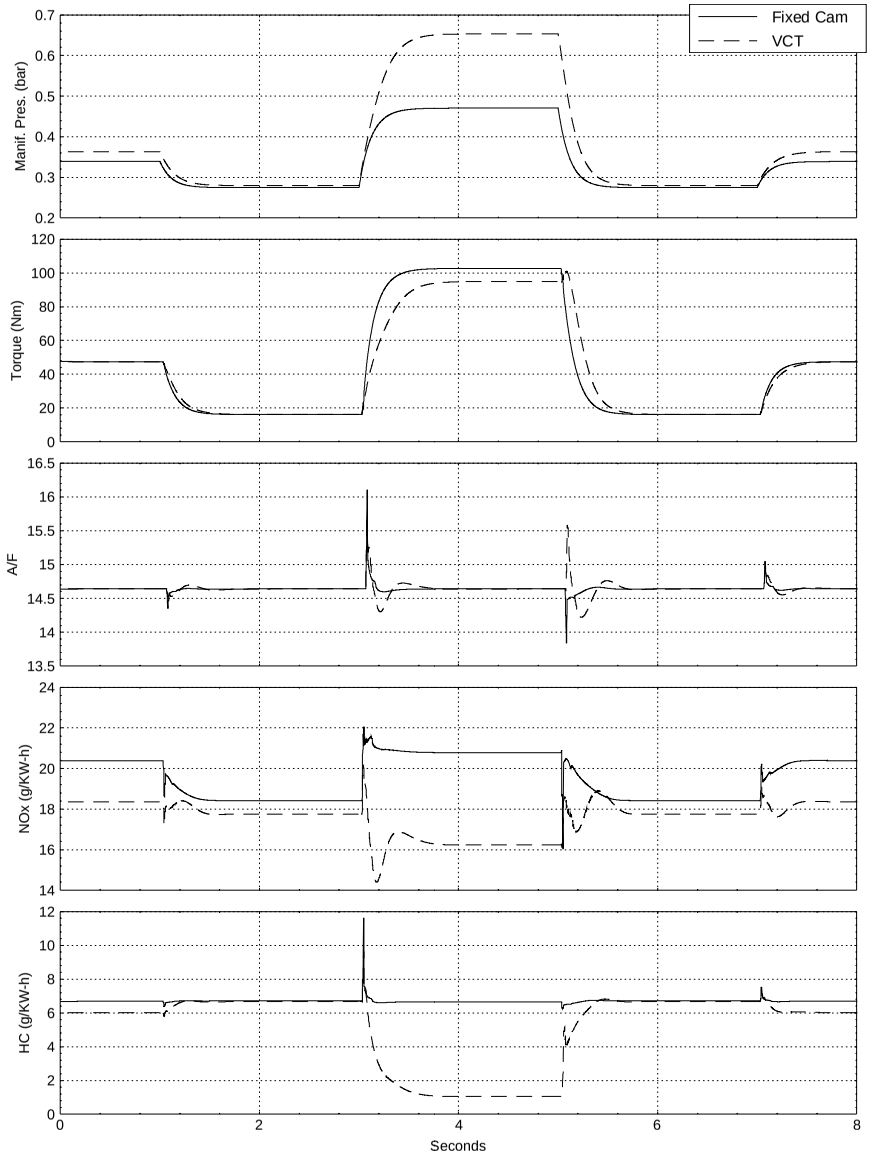

Figure 8: Simulation response of the conventional and the VCT engine.

Figure 9: Simulation response of the multivariable and the PI control scheme